Synopsis

Design, Synthesis and Properties of Novel Oligo-Phenylenevinylene based Supramolecular Photochromic Gels and Soft Composites with Nanomaterials

The thesis entitled **"Design, Synthesis and Properties of Novel Oligo-Phenylenevinylene based Supramolecular Photochromic Gels and Soft Composites with Nanomaterials"** deals with soft materials derived from low molecular mass photochromic gels and nanomaterials.

Chapter 1 gives a general introduction and overview of the low molecular mass gel (LMMG). It briefly delves into the history of research in physical gel field, design of different types of photochromic gelator molecules, their interesting self-assembly patterns, potential applications of these gelator molecules as well as challenges to design of new gelator molecules. A comprehensive discussion on the synthesis and numerous applications of smart nanocomposites derived from LMMGs and nanomaterials were discussed. It also encompasses the relatively recent area of two component gel system to conveniently bypass the cumbersome synthetic protocol. Interesting photophysical properties of these photochromic LMMGs were discussed towards their light-harvesting properties and aggregation induced white-light emission.

Chapter 2 describes the synthesis and self-assembly properties of all-trans-tri(p-phenylenevinylene) (TPV) based molecules possessing different terminal groups, *e.g*. oxime, hydrazone, phenylhydrazone and semicarbazone (Chart 2A.1). Various spectroscopic and microscopic studies show the aggregation pattern of the self-assemblies promoted by hydrogen bonding, aromatic π-stacking and van der Waals interactions among the individual TPV units (Figure 2A.1). The melting temperatures of the gels and viscoelastic behaviour indicate that the presence of more hydrogen-bonding donors in the periphery of the gelator molecules makes the gel thermally and mechanically more robust. However, in the presence of more numbers of hydrogen-bonding donor/acceptors at the periphery of TPVs such as with semicarbazone a precipitation as opposed to gelation was observed. Thus, the choice of the end functional groups

and the number of hydrogen-bonding motifs in the TPV backbone holds the key and modulates the effective length of the chromophore, resulting in interesting optical properties.

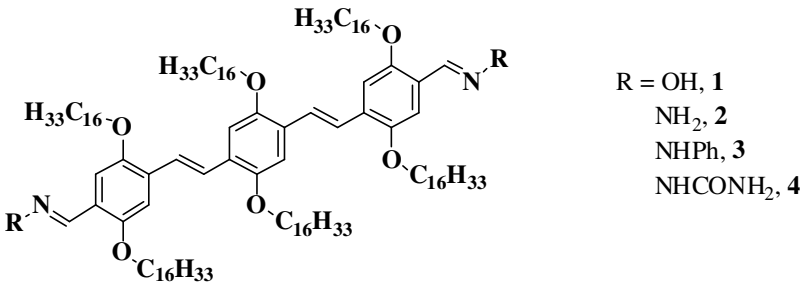

Chart 2A.1. Molecular structures of various TPV based gelators.

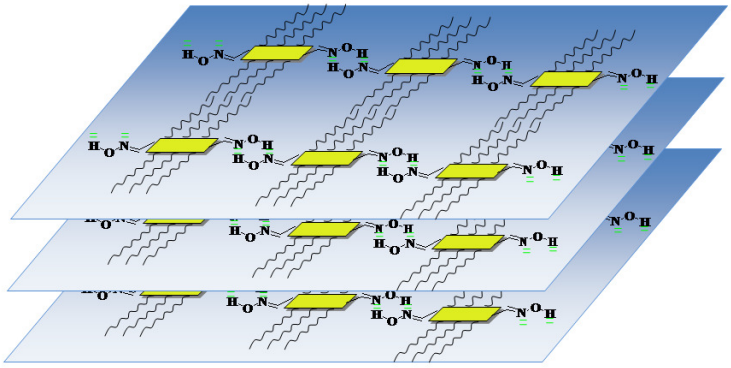

Figure 2A.2. Proposed model depicting π–stacking, hydrogen bonding and van der Waals interactions among the TPV units in **1**.

Chapter 3A demonstrates successful incorporation of pristine and long-chain functionalized single-walled carbon nanotubes (SWNTs) in supramolecular organogels of **1** (Chart 2A.1) to give rise to new nanocomposites with interesting mechanical, thermal and electrical properties (Figure 3A.1). The SWNT promoted aggregation of **1** leads to quenching of the absorption and emission intensity of **1**, increases the sol-to-gel transition temperature and increases the viscoelasticity of the composite gels. The composites were semiconducting in nature and showed enhanced electrical conductivity compared to that of **1** alone. Upon irradiation with a near IR laser at 1064 nm for 5 min, it was possible to selectively induce a gel-to-sol phase transition of the nanocomposites, while irradiation for even 30 min of the native organogel under identical conditions did not cause any gel-to-sol conversion.

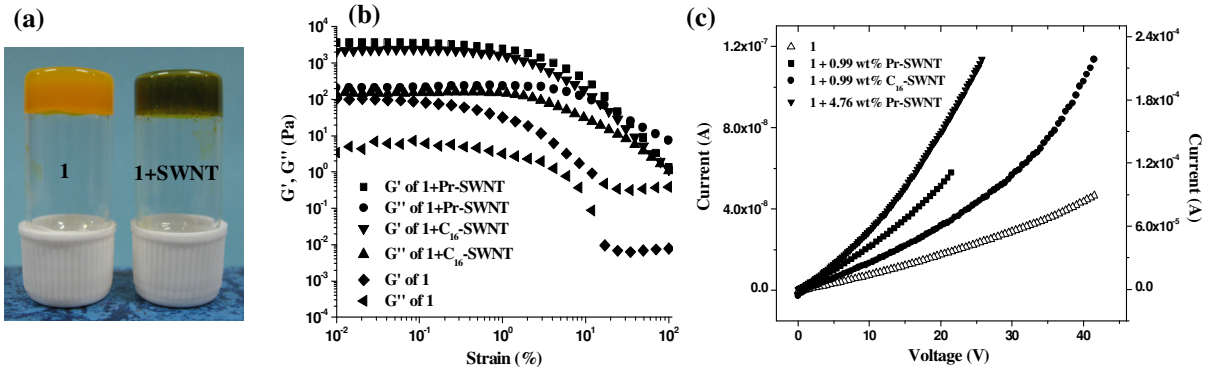

Figure 3A.3. (a) Photograph of toluene gel of **1** and its composite with Pr-SWNT, (b) oscillatory amplitude sweep experiments of toluene gel of **1** (5 mg/mL) alone and **1**+Pr-SWNT (0.25 wt%). (c) *I-V* measurements of **1**, **1**+0.99 wt% Pr-SWNT, and **1**+0.99 wt% C_{16}-SWNT (left Y-axis) and right Y-axis show current of **1**+4.76 wt% Pr-SWNT.

Chapter 3B describes incorporation of multi-walled boron nitride nanotubes (BNNTs) and various functionalized BNNTs by Lewis bases such as trioctylamine (TOA), tributylamine (TBA), and triphenylphosphine (TPP) in the toluene gel of **1** (Chart 2A.1). Functionalized BNNTs were synthesized first and incorporation into the gel showed evidence of wrapping of the gelator molecules on to the BNNT surface presumably brought about by π-π stacking and van der Waals interactions (Figure 3B.1). This leads to the formation of densely packed and directionally aligned fibrous networks. Such "reinforced" aggregation of the gelator molecules in presence of doped BNNTs led to an increase in the sol-to-gel transition temperature and the solidification temperature of the gel-nanocomposites as revealed from differential scanning calorimetry. Rheological investigations of the gel-nanocomposites indicate that the flow properties of the resulting materials become resistant to applied stress upon incorporation of even a very low wt% of BNNTs. Finally, the increase in thermal conductivity of the nanocomposite compared to the gelator alone was observed for the temperature range of 0-60 ^{o}C which may make these composites potentially useful in various applications depending on the choice and the amount of BNNT loading in the composite.

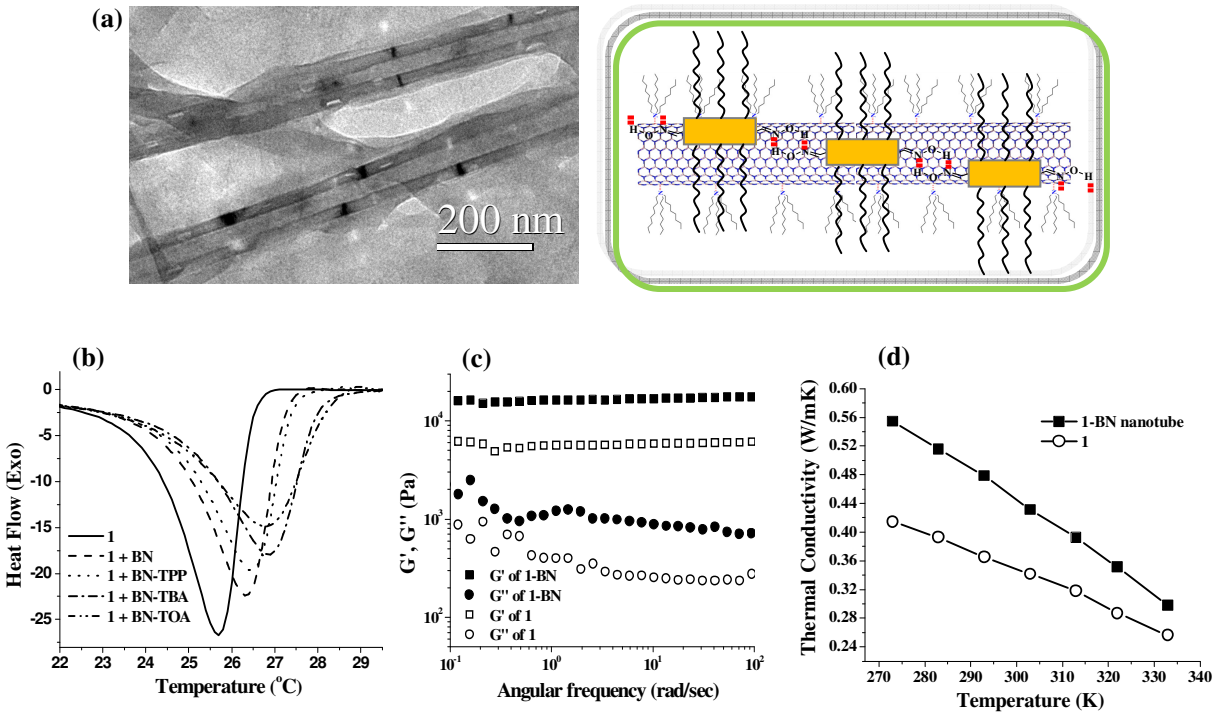

Figure 3B.4. (a) Wrapping of **1** on BN nanotube under TEM and proposed mode of interaction. (b) DSC and (c) rheology of toluene gel of **1** (10 mg/mL) and **1**+BNNTs (0.83 wt%). (d) Thermal conductivity of the xerogel of **1** and **1**+BNNT (10 wt%) composite films as a function of temperature.

Chapter 3C presents first successful incorporation of graphene, and long aliphatic chain (*n*-dodecyl, *n*-hexadecyl) functionalized graphene in physical organogels formed by the aromatic oligo-phenylenevinylene (OPV) based gelator **1** (Chart 2A.1) and (non-aromatic) amino acid derived gelator. The large aromatic surfaces of gelator **1** serve as a host matrix for the incorporation of graphene and other nanocarbons (fullerene, SWNT). Such carbon nanomaterials (CNMs) exerted variable effects on the gelator through non-covalent interactions, due to their differences in shapes. Various microscopic images confirm the formation of densely wrapped fibrous networks for the resulting nanocomposites upon incorporation of CNMs. Variable temperature UV-vis and fluorescence spectra reveal CNMs mediated aggregation of the gelator molecules in solution and the presence of supramolecular interaction was evident from Raman spectroscopy. This 'reinforced' aggregation of the gelator molecules on doped CNMs was reflected in significantly enhanced thermal, mechanical and electrical properties of the nanocomposites. Rheological investigations of gels containing small amount of CNMs indicated that the flow of nanocomposites became resistant to applied stress at a very low wt-% of CNM incorporation (0.83 wt-%). An interesting synergistic behaviour was observed in case

of the composite gel of OPV based LMOG containing a mixture of EG and SWNT when compared with other mixtures of CNMs in all combinations with EG. These studies are therefore of great contemporary interest as they provide molecular level control into the preparation of novel nanocomposites of LMOG and nanocarbons.

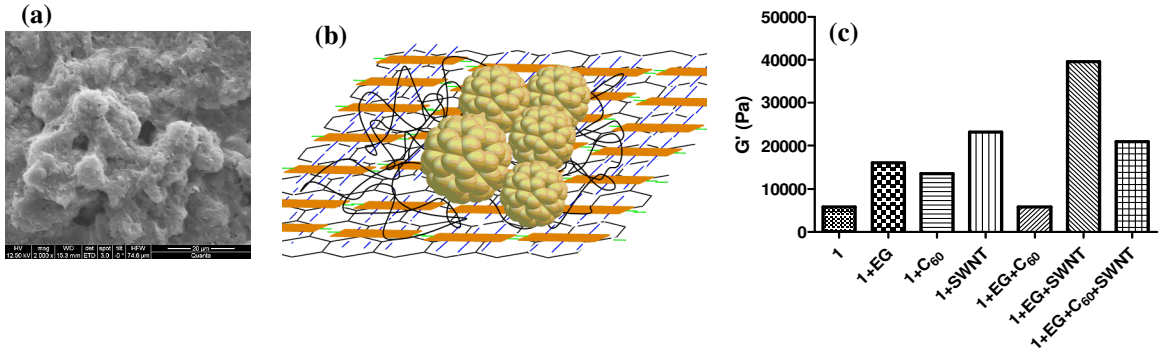

Figure 3B.5. (a) SEM image of **1**+EG+C_{60}+SWNT showing close proximity of the wrapped CNMs by **1** as depicted by the proposed model in (b). (c) The G' value of the gels of **1** (10 mg/mL) with CNMs and mixtures of CNMs (0.83 wt% CNMs were added individually).

Chapter 4 describes the synthesis of two low molecular mass organogelators based on tri-*p*-phenylenevinylene derivatives one of which could be designated as "acceptor" while the other one as "donor" (Figure 4.1). These were prepared specifically to show the inter-gelator interactions at the molecular level between each other through the donor-acceptor type of assembly to achieve control over their macroscopic properties. Intermolecular H-bonding, π-stacking and van der Waals forces are operational for both the individual and the mixture leading them to the gel formation in chosen organic solvents.

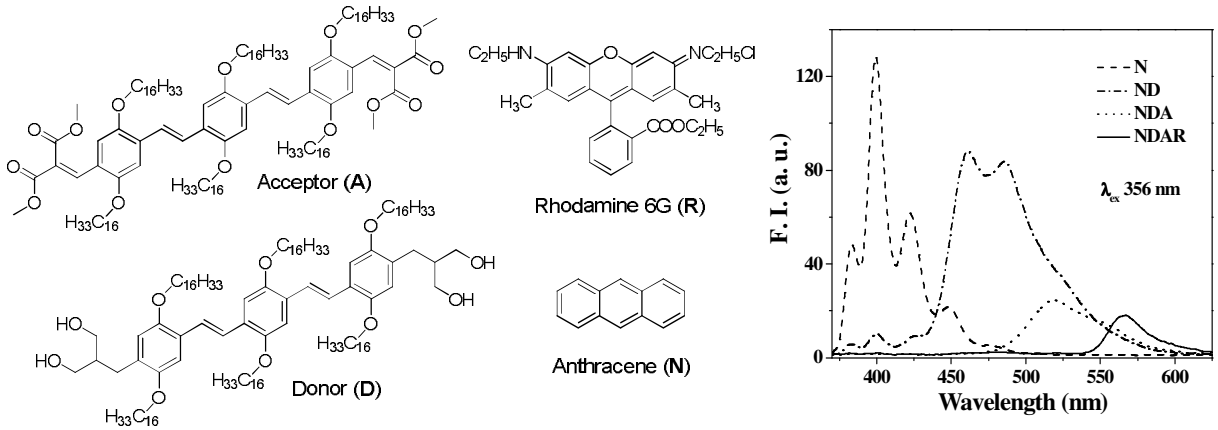

Figure 4.1. Molecular structures of the donors and acceptors involved in the cascade energy transfer.

Due to the photochromic nature of this class of molecules, they exhibited interesting photophysical properties. An efficient energy transfer was demonstrated from the mixture of donor-acceptor assemblies in solution. An array of four chromophores was built up by including two known dyes *i.e*. anthracene and rhodamine 6G for the energy transfer studies. Interestingly a cascade energy transfer was observed in the assembly of four chromophores in the series. This allowed building up of a wide range of light harvesting process, excitation at one end of which produces an emission at the other end of the assembly.

Chapter 5A discusses the synthesis of new dicationic chromophoric phenylenedivinylene bis-N-alkyl pyridinium salts to study their hydrogelation behaviour through π-stacking and van der Waals interactions (Figure 5A.1). A crucial hydrophilic-hydrophobic balance in aqueous medium controls the gelation when a specific length of the aliphatic chain (*n*-octyl, **2**) is appended on the both ends of the central aromatic core. The hydrogels showed considerably high gel-melting temperature and more viscoelastic solid-like properties with increasing concentrations of the gelator **2**. Microscopic studies exhibited concentration dependent mixed fiber-coil morphology above its gelation concentration and only fibrillar networks below the gelation concentration (Figure 5A.1). Variable temperature, UV-visible and fluorescence spectroscopy showed aggregation induced emission switches for the self-assemblies promoted by addition of various salts (either cations or anions) in diluted solutions. Aggregation induced white-light emission could be achieved in aqueous medium either by tuning the concentration of the added salt or by varying the temperature of the mixture. Cyclic-voltametric studies indicate a reversible one-electron redox behavior for the chromophore which is also diffusion-controlled in nature. Lamellar type arrangement in the self-assembly was evident from the X-ray diffraction analysis. Gradual downfield shift in the proton signals of the ^{1}H-NMR spectra upon heating suggest aromatic π-stacking and van der Waals interactions are operational among the gelator molecules and a balance with the electrostatic interactions lead to the physical gelation in water.

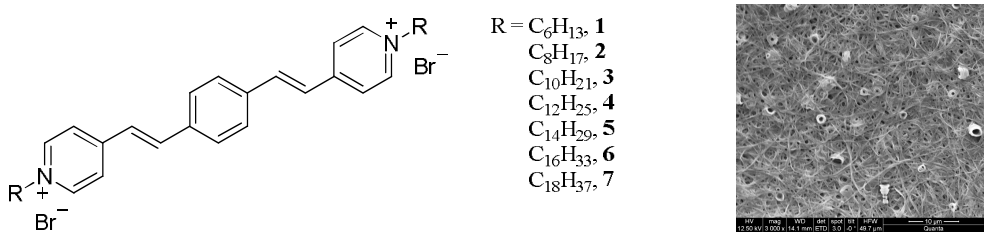

Figure 5A.1. Molecular structures of the dicationic analogues and the fiber-coil morphology of gels.

Chapter 5B presents supramolecular π-gel formation by phenylenedivinylene bis-N-alkyl pyridinium salts appended with terminal aliphatic hydrocarbon chains of different lengths (Chart 5A.1) in specific ratios of aliphatic alcohols and water mixture. The temperature- and the ratio-variation in the ethanol/water mixture showed the aggregation pattern of the self-assemblies promoted by electrostatic, aromatic π-stacking and van der Waals interactions among the individual gelators as observed under UV-visible and fluorescence spectroscopy. With increase in the number of carbon atoms in the aliphatic chain, greater gel-melting temperature, increased viscoelastic solid-like behavior and decreased fiber diameter was observed among the gelators. However, presence of excess hydrophobic moiety at the periphery, a precipitation as opposed to gelation was observed. Cyclic-voltametric studies show a one-electron reversible redox behavior for the chromophore and the redox potential decreases with increasing the aliphatic chain length. A diffusion-controlled redox behavior was observed for shorter aliphatic chains but the longer chains make the process diffusion-limited. The electrical conductivity studies show semiconducting behavior for individual compounds and the magnitude of current increases with increasing fiber diameter (with decreasing aliphatic chain length).

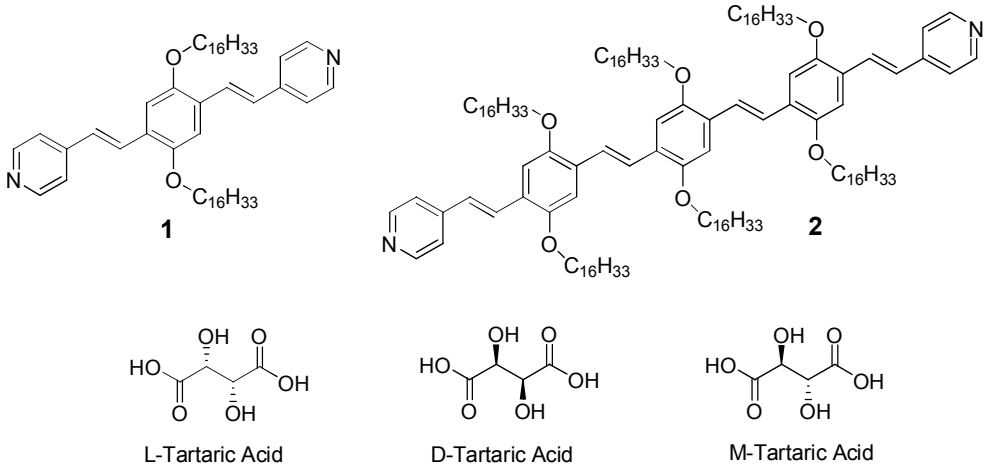

Chart 6A.1. Molecular structures of the pre-gelator **1** and **2** and three different tartaric acids undertaken for the gelation studies.

Chapter 6A demonstrates the synthesis of new oligo-phenylenevinylene (OPV) analogues with pyridine end-functionality (Chart 6A.1) to show efficient supramolecular organogel formation through molecular complexation with tartaric acids (TA). The salt formation between the end-pyridine and TA exhibited a significant decrease in the IR stretching frequency of the carboxylic

acid. Microscopic studies showed a nucleation induced growth of the fibers that essentially led to larger aggregate formation. A circular dichroism study demonstrated an opposite sense of chirality in the complexes for two optically active TA (L and D). The expression of chiral transcription in the achiral OPVs was manifested under atomic force microscopy which showed a specific handedness in the fibers for the complex with particular optically active TA. Fluorescence spectroscopic studies exhibited a remarkable red-shift of the emission maxima due to the *J*-type aggregation leading to the gel formation. In a particular condition, energy transfer from aggregated donor to aggregated acceptor was observed in the gel phase. A liquid crystalline behavior was observed under polarized optical microscopy as well.

Chapter 6B describes selective Hg^{2+} sensors which have been achieved separately under 'naked eye' and fluorimetric method for two-coordination assisted conjugated pyridine-end oligo-phenylenevinylene moieties (Chart 6A.1, **1** and **2**). A drastic visual color change was exhibited based on the conjugation length of such chromophores. The visual color change was more prominent in the chromophore containing five aromatic rings in a conjugation compared to only three aromatic rings. However, breakdown of the conjugation length in the chromophore unit through incorporation of semicarbazide moiety (isoniazid) (Chart 6B.1) leads to a lesser degree of change either visually or spectroscopically. Coincidently, the isoniazid moiety provides an extra motif for their anion sensing properties through the deprotonation of 'N-H' group. Thus a selective CN^- sensor was achieved. The presence of H-bonding donor (-NH-) and acceptor (-CO-) group in the semicarbazone segment and the long *n*-hexadecyl chains induced a physical gel formation. Addition of Hg^{2+} or CN^- to the gel leads to the gel-to-sol transition and further addition in a reverse order could induce a reversible gel formation. Effect of addition of Hg^{2+} and CN^- to the gel was probed by UV-vis and ^{1}H-NMR spectroscopy which showed significant spectral shifts in favor of their interactions.

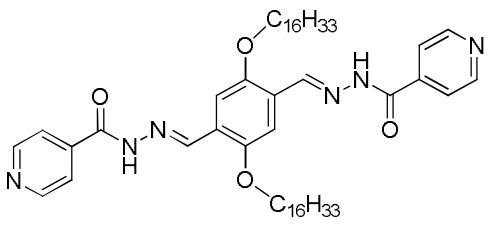

Chart 6B.1. Molecular structure of the chemosensor for the sensing of both Hg^{2+} and CN^- ions.